Stability Diagram of upper flow regime bedforms. An experimental study

Master thesis W.J.R. Poos
Universiteit Utrecht
November 2011

Abstract

Water flowing over a bed made of silici-clastic material forms bedforms. A stability diagram for these bedforms is available for the lower flow regime where the Froude number < 0.8. No such diagram is available for the upper flow regime ($Fr > 0.8$). Experiments in a tiltable flume show that the bedforms for the upper flow regime can be characterized as: upper plane bed, antidunes, chute and pools and cyclic steps. These bedforms are plotted in a stability showing the relation between the dimensionless grain size and the ratio of minimum and maximum Froude number (before and after the hydraulic jump if present) showing proof of concept for such a stability diagram.

1. Introduction

Paleo flow conditions are stored in the fossil record by the bedforms that are formed by these conditions. Water flowing over a non-cohesive sedimentary bed shapes it and leaves bedforms such as ripples and dunes. Specific flow conditions leave behind specific bedforms. These bedforms can be represented in a stability diagram to show the stability relations of the different bedform phases .

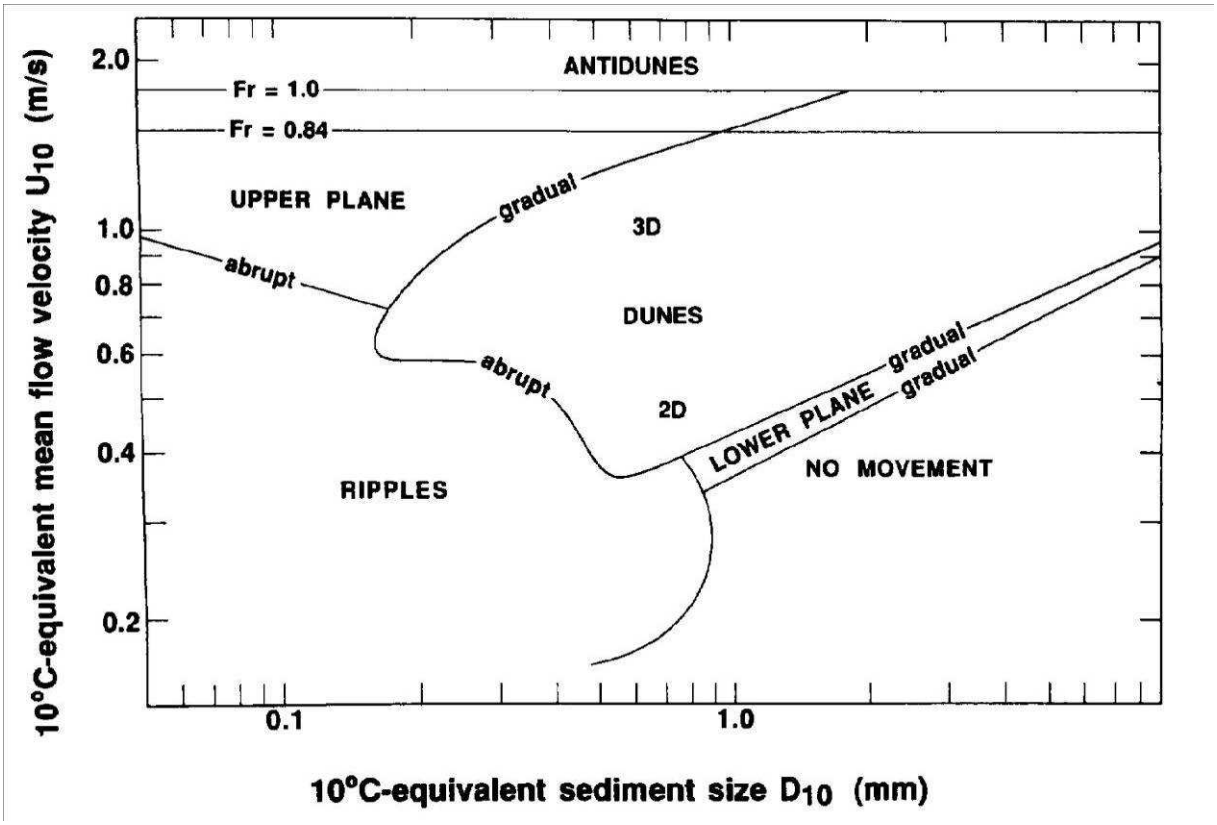

Figure 1 *Stability diagram of Southard and Boguchwal (1990) which is more directly suitable for field use. The upper flow regime is represented in the upper part of the diagram as the Fr = 0.84 and Fr = 1.0 lines*

Stability diagrams that characterizes the different flow conditions for common bedforms come in several varieties; diagrams based on a grain related roughness parameter and dimensionless grain size (Van den Berg &Van Gelder 1993) (Figure 2) or based on dimensionless measures of flow depth and grain size (Southard & Boguchwal 1990) (Figure 1). Both use dimensionless parameters that describes the flow on the ordinate and the bed on the abscissa. These diagrams are well suited for the lower flow regime. They do extend into the upper flow regime but do not distinguish between upper flow regime bedforms. The focus of this thesis lies on these upper flow regime bedforms.

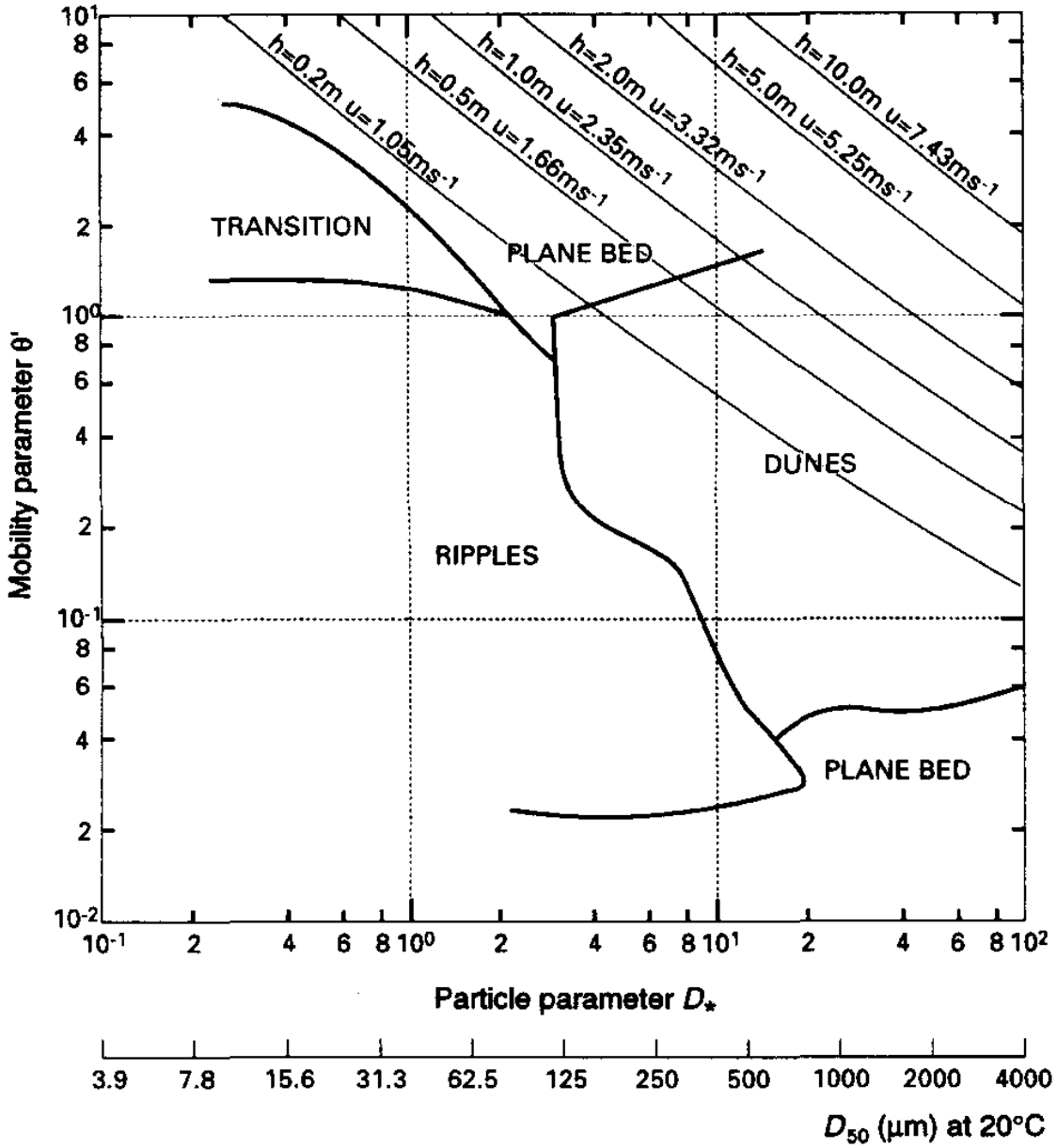

Figure 2 *Stability diagram of van den Berg and van Gelder (1998) based on a grain related roughness parameter and dimensionless grain size. The upper flow regime is represented by the Froude=0.75 lines plotted in the upper part of the diagram. This is the limit of antidunes formation for several depths and corresponding flow velocities. There is no distinction between different upper flow regime bedforms in this diagram*

The different flow regimes are defined by the phase of the bedform elevation and the water surface. In the lower flow regime, the elevation of the bedforms is in antiphase with the water surface. In the upper flow regime this is the other way around (Simons and Richardson 1966). The upper flow regime has a Froude number higher than 0.75-0.8.

The Froude number (*Fr*) describes the criticality of the flow and is defined by

$$Fr = \frac{\bar{u}}{\sqrt{gh}} \qquad (1)$$

for subaerial conditions of water flow as first described by Jean-Baptiste Bélanger (Bélanger 1828), where $\overline{u}$ is the depth-averaged flow velocity, g is the local acceleration of gravity (9.81 m/s^2) and h is the waterdepth. The Froude number is the ratio between the flow velocity ($\overline{u}$) and the wave velocity ($g*h$). This means that if the $Fr < 1$ the flow is subcritical and downstream disturbances affect upstream conditions (the backwater effect (Yarnell 1934)) and behaves as a fluvial flow. If $Fr > 1$ the flow is supercritical and behaves like a torrential flow. Downstream disturbances do not affect upstream conditions. This manifests itself in the raising of the water level upstream of any disturbance. A direct result from this is the phenomena of the hydraulic jump.

These jumps occur when fast flowing, shallow, supercritical flow rapidly transitions into deeper, calmer, subcritical flow. The subcritical part of the flow is subject to the backwater effect, causing the water level to rise due to the obstacle of slower flowing water downstream. The supercritical part is not subject to this effect which means that at the transition of supercritical to subcritical flow the backwater effect manifests itself and a rapid rise in the water level results. The presence of hydraulic jumps is the most important aspect of the upper flow regime since these jumps occur on the transition from supercritical to subcritical flow and supercritical flow only occurs in the upper flow regime. The difference between the upper flow regime and supercritical flow is that the latter is confined to the former but the upper flow regime does not consist solely of supercritical flow.

The conditions of the upper flow regime result in a different interaction between bed and flow. The bedforms that form under these conditions are called: antidunes, breaking antidunes, chutes-and-pools and cyclic steps (Taki&Parker2005 Simons 1965, Gilbert 1914). These bedforms are described below:

- **Upper plane bed.**
  Flat bed that can form laminations in an aggradational environment. In our experiments, erosion was equal to sedimentation and no internal laminae formed. This type of bedform forms at $Fr > 0.7$ (Figure 3A).
- **Antidunes**
  Antidunes usually migrate upstream. Water surface elevation mimics the elevation of the bed, also in contrast to normal dunes where the water is slightly depressed just above the top of a dune. The elevation over the crest is higher than the depression over a trough. This creates near-bed flow deceleration from trough to crest and acceleration from crest to trough. Net deposition will occur upstream of the crest and net erosion downstream of the crest, such that the antidunes tend to migrate upstream.(Carling 2002) This situation is occasionally reversed (Fukuoka 1982). The resultant bedforms resemble antidunes but migrate downstream. This situation only occurs when $Fr < 1$ (Figure 3B).
- **Breaking antidunes**
  Breaking antidunes are a step up from normal antidunes in the sense of supercriticality. Water flow loses enough velocity while travelling up the stoss side of a breaking antidune to become subcritical. This initiates a (small) hydraulic jump at the crest of an antidune. This is a preliminary form of chute and pools. These were not studied during the experiments due to the ephemeral nature of the hydraulic jump in this type of bedform (Figure 3C).
- **Chute and pools**
  Chute and pool flow consists of a long chute where Froude number > 1. The chute terminates in a hydraulic jump. A 'pool' forms directly downstream from the jump. Here the flow is subcritical but accelerating, until it becomes supercritical again and the next chute and pool form. The distance between hydraulic jumps differs over the length of the entire flow. (Figure 3D).

-**Cyclic steps**

These bedforms consist, just like in the chute and pool morphology, of a ramp where the flow accelerates, followed by a hydraulic jump and a tranquil pool where flow is subcritical. This is followed by the next ramp. The main difference between cyclic steps and chute and pools is the wave length of cyclic steps is roughly constant over the length of the flow (Figure 3E).

A comprehensive, distinctive stability diagram for the upper flow regime is still lacking. Flow conditions that incorporate hydraulic jumps are inherently unsuitable for plotting in the existing flow diagrams. Van den Berg and Van Gelder (1998) does show the lower limit for antidune formation for several depths in his stability diagram but this does not cover the entire range of upper flow bedforms since only antidunes are taken into account. In addition, the parameter on the ordinate is the grain related mobility parameter θ' and is defined by

$$\theta' = \frac{\rho \bar{u}^2}{(\rho_s - \rho)(C')^2 D_{50}} \qquad \textbf{(2)}$$

with

$$C' = 18\log\left(\frac{4h}{D_{90}}\right) \qquad \textbf{(3)}$$

where ρ_s is the sediment density, ρ is fluid density, D_{50} is the median grain size of the bed material and D_{90} is the 90th percentile of the grain size of the bed material. In the case of the diagram by Southard and Boguchwal (1990) the parameter on the ordinate is 10° C-equivalent mean flow velocity which also depends on $\bar{u}$, making it unsuitable for the upper flow regime. It is inherently impossible to plot these bedforms into that stability diagram due to the fact that both h and $\bar{u}$ vary heavily along the length of the bedform. Hence, existing stability diagrams, which can not compensate for variable flow conditions along the length of the flow, are unsuitable for upper flow regime bedforms.

The aim of this thesis is the establishment of a stability diagram incorporating dimensionless parameters to characterize upper flow regime bedforms.

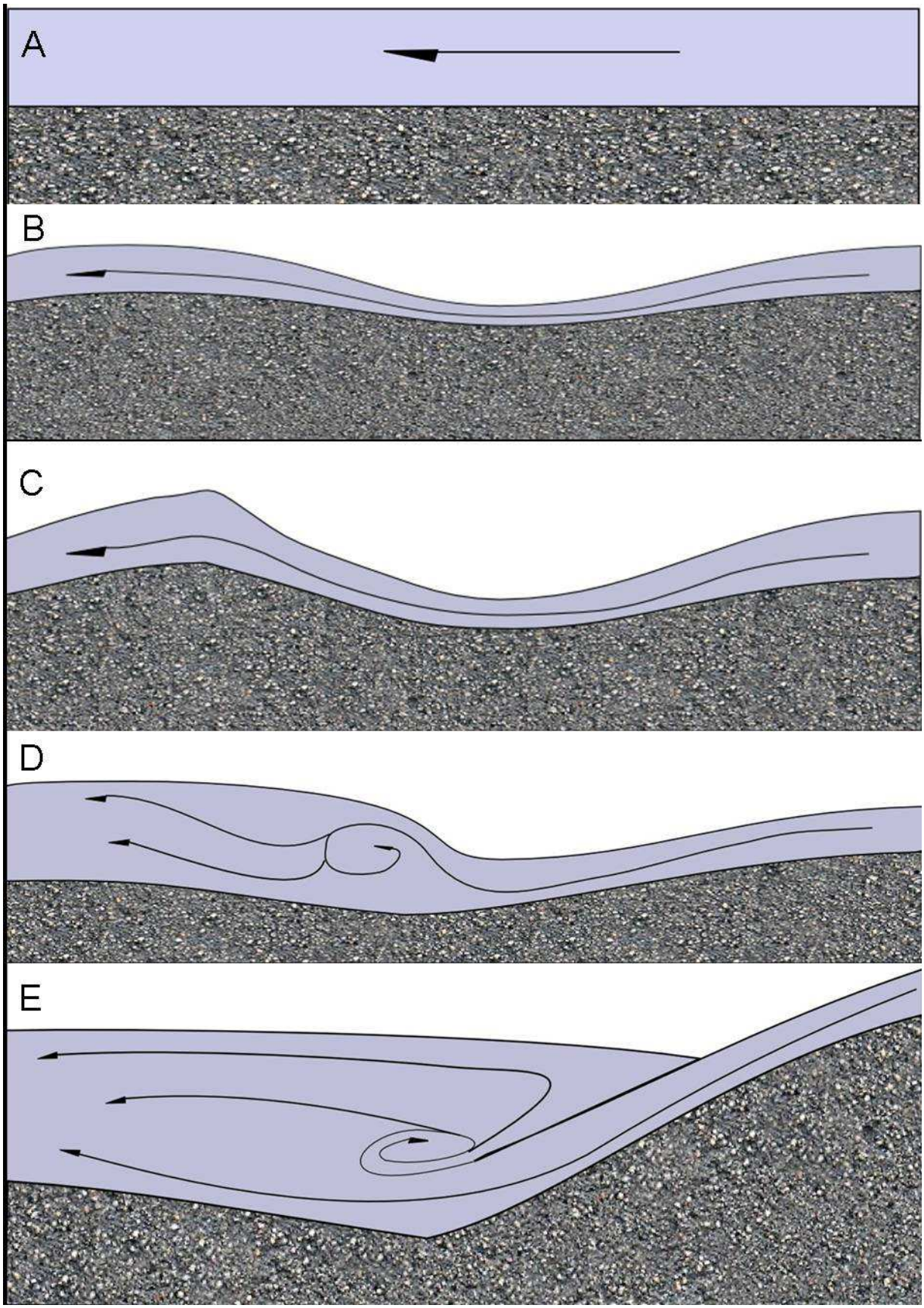

Figure 3 *Bedforms of the upper flow regime, A: Upper plane bed, B: Antidunes, Bedform migrates upstream, no hydraulic jump occurs, C: Breaking antidunes, Hydraulic jump occurs, D Chute and pools, E Cyclic step.*

3. Methods and materials.

The experiments were done in a recirculating flume that can be tilted up to 10° (Figure 4, Figure 6). Water and sediment flowing out at the downstream end were circulated to the upstream end. The flume used is 12 meters long and 0.485 meters wide (Figure 4 and Figure 6). The width of the flume is sufficiently small compared to the length to assume 2-dimensional flow Water and sediment were pumped into a reservoir at the upstream end from which the mixture flows into the flume to minimize the rotational effect of the pump.

The formation of upper flow conditions requires a relatively steep slope (>0.05m/m). This is done by using the pump to create a large hydraulic head difference between the upper and lower portion of the flume The tilting of the flume is important since it allows stable bedform formation at much steeper slopes (Figure 5).

Upper flow regime bedforms need a sufficient overall slope to form. It is possible to create such a slope during experiments by piling up sediment at the upper end of the flume. Why this does not work is explained here: When there is a hypothetical barrier at the outflow section of the flume, the pump is used solely to establish a hydraulic head at the outflow end of the flume. Discharge through the pump is effectively zero. When the barrier is lowered (B, C) the hydraulic head gets lower and discharge increases. Discharge will continue to increase until the barrier is gone. At that point all the power of the pump is used to pump water around and establish a sufficient elevation at the upstream end for the water to overcome the roughness of the flume and keep flowing. (D). When this barrier is formed by a pile of sand (E) the greatest amount of erosion takes place at the arrow causing much of the sediment to be distributed over the rest of the flume (F). This prevents upper flow regime conditions due to lowering of the overall slope. If the flume is tilted (C), then the wall of the flume, which is made of steel and therefore highly erosion resistant makes up part of the barrier. This creates a stable situation where sediment covers the entirety of the bottom of the flume.

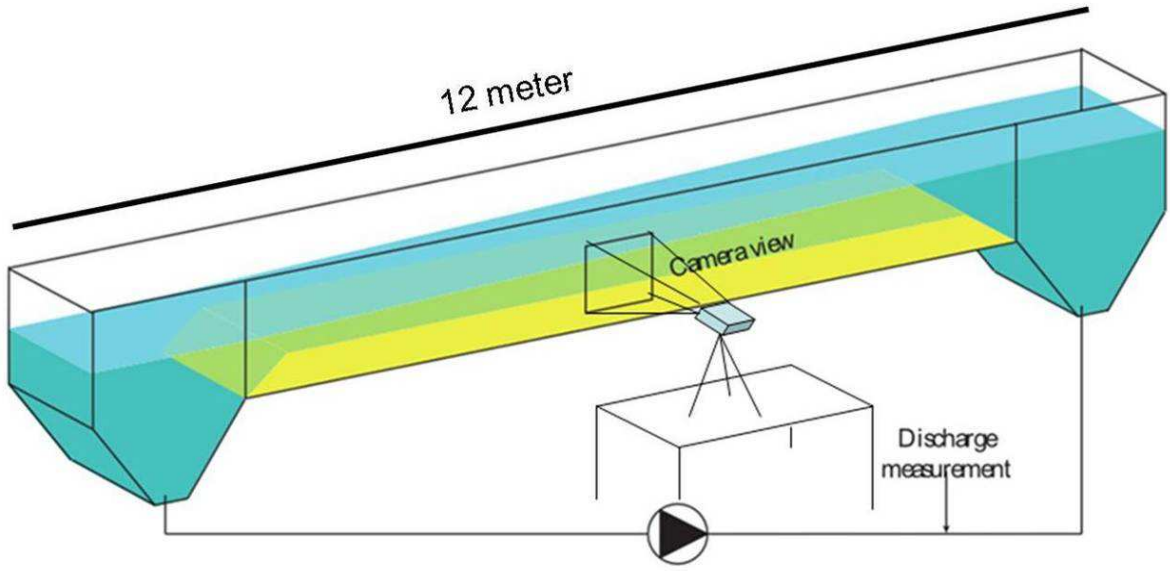

Figure 4 *Diagram of the recirculating flume*

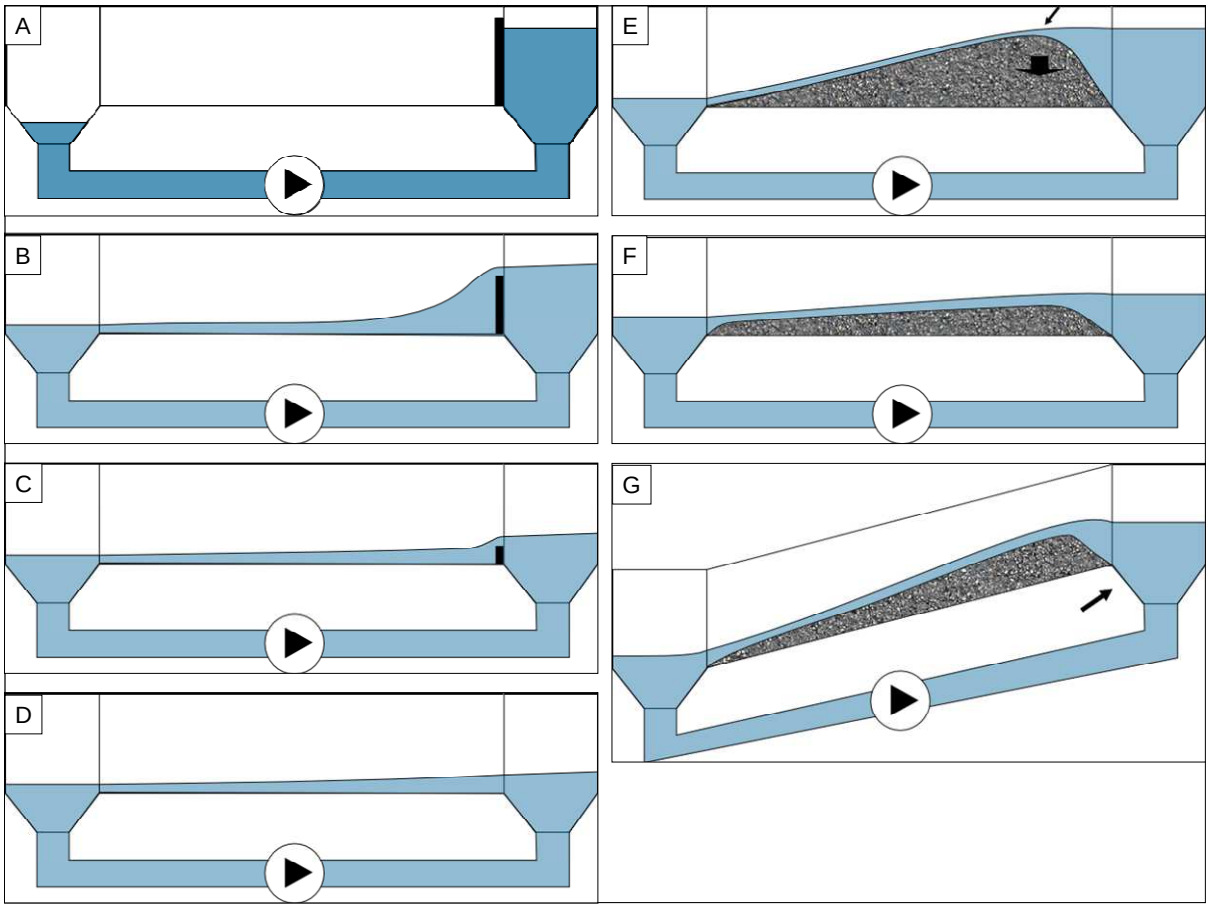

Figure 5 *Cross-section of the pump is represented by the arrow in the circle.*

Figure 6 *Flume used in the experiments during a run establishing cyclic steps, the vertical bars are spaced at 1 meter*

Two types of sediment were used in the experiments. One (sediment 1) is a well-sorted silici-clastic sand with a D_{50} of 190 μm as determined by laser diffraction. The other (sediment 2) is a poorly sorted, bimodal, silici-clastic sand with a D_{50} of 425 μm as determined by sieve analysis. The grain size distributions are shown in Figure 7.

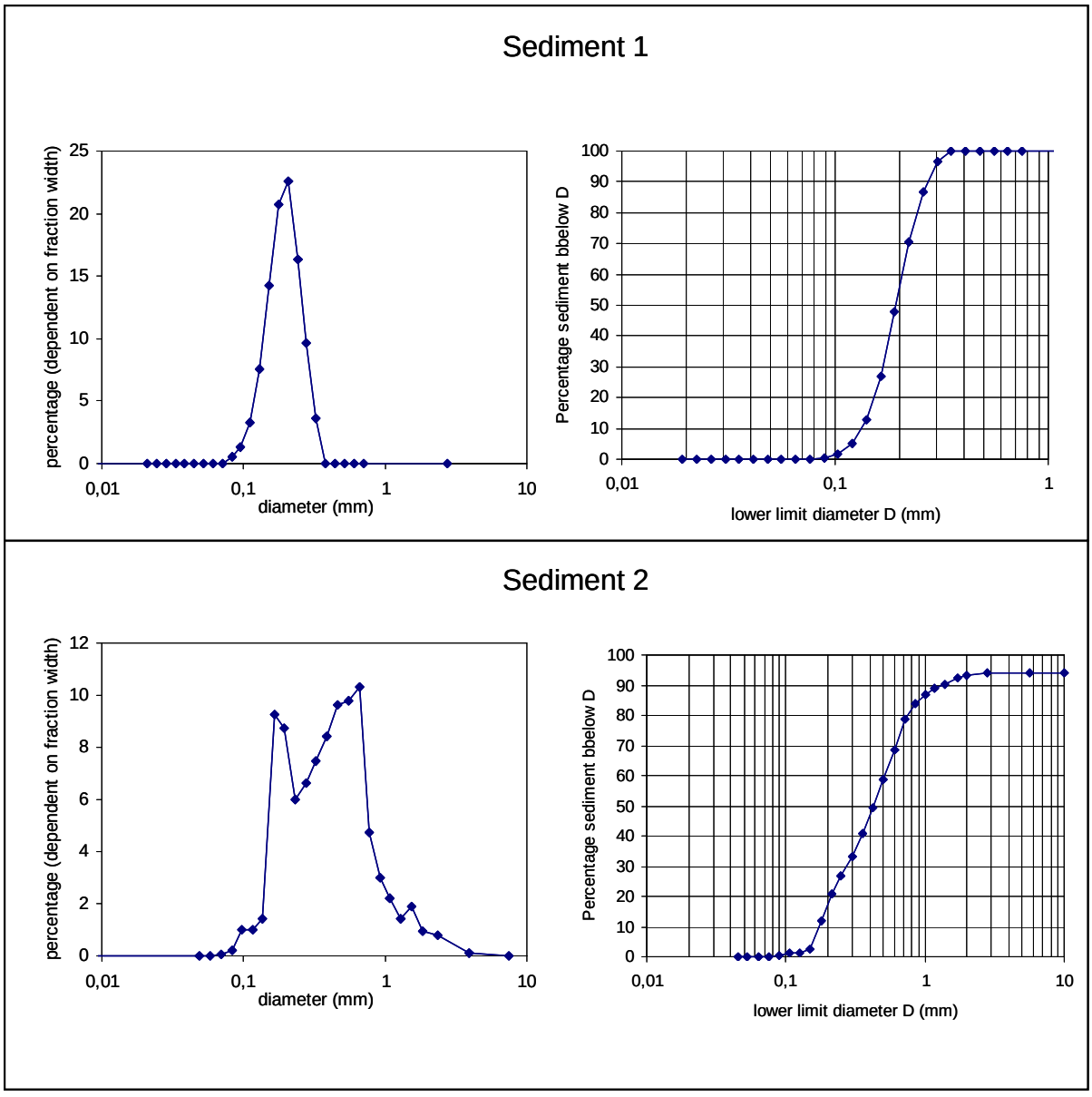

Figure 7 *Grain size distribution of the two different sediments used in the experiments.*

We continuously monitored a section of the side of the flume using a high-speed camera that took a picture every 0.1 sec.

For the parameter to describe the bed we use the non-dimensional particle parameter D* as introduced by Bonnefille (1963). This is defined as (4).

$$D^* = D_{50}\left(\frac{(\rho_s - \rho)g}{\rho\nu^2}\right)^{\frac{1}{3}} \qquad \textbf{(5)}$$

there ν = the kinematic viscosity, 0.000101 at room temperature (20° C). This parameter is used because, like the Froude number, it is dimensionless and can be easily reduced to the median grainsize.

4. Results

Before any measurement was done on the flume several trial runs were made. These runs were used to determine the proper settings for stable configurations of the flume. The main problem encountered during these trial runs consisted of the flow scouring the bed in such a degree that the bottom of the flume was excavated. This would result in unnatural wavelengths of the bedforms. To solve this problem required a balance between four factors: tilting of the flume, power of the pump and amount of sediment and the amount of water in the flume.

1. If the flume was not tilted in the correct way to create a balanced bed foundation the flow would erode all the way to the bed at either the upstream end (too steep) or the downstream end (not steep enough).

2. Power of the pump determined both the hydraulic head difference as well as the discharge through the system. Both have to be sufficient to create upper flow bedforms but not too large to initiate complete erosion at some locations.

3. The amount of sediment/water in the flume also determined the success of a trial run. Too much sediment and the flume would overflow, too little and the bottom of the flume would be excavated.

4. The amount of water determined the criticality of the flow. This is highly dependent on water depth and less water usually means higher Froude numbers. This works until there is so little water in the flume that it can no longer cover the entire width of the flume and 3-dimensional effects start to play a role. This last is less than desirable. These problems were solved by adding more sediment to the flume to decrease the change of excavation as well as removing just enough water to prevent 3D-effect from forming.

These trial experiments resulted in stable conditions of different types of bedforms At the beginning of each run the power of the pump recirculating the material was set at a fixed level. This setup was then allowed to continue until equilibrium in the type of bedform was reached by checking the height of the passing bedforms and ensuring that they did not scrape the bottom of the flume at either end. A total of 14 runs were made. In one run an upper plane bed was established. This was done specifically to test the set-up for measuring velocity (Appendix 1) and to get another control point in the linking of stability diagrams. Three runs were set up so that no hydraulic jumps formed. Five runs which did include hydraulic jumps but differed in the distance between the hydraulic jumps. Five runs were made that both included hydraulic jumps as well as a constant distance between the hydraulic jumps. This setup corresponds roughly to antidunes (no hydraulic jump), chute and pool (hydraulic jump but variable wavelength) and cyclic steps (hydraulic jumps and constant wavelength), respectively, from the classification by Taki and Parker (2005) and Alexander (2001). The experimental runs are summarized in Table 1 and shown in Figure 8.

Bedforms

As the flow starts to become supercritical, small irregularities cause the supercritical flow to slow down at that specific point. Here a bedform starts to form. Flow velocity increases at its lee side due to an increase in slope It slows down at the stoss side of the next antidune, again due to change in slope. This means erosion takes place at the lee side and deposition at the stoss side, causing the bedforms to migrate upstream. Flow does not become subcritical again at the top of the dune. No hydraulic jump occurs (Figure 8A)

If the energy of the system increases even further the erosion at the lee side increases as well as the deposition at the stoss side. The increase in height of the next bedforms causes the flow to slow down to such an extent that a hydraulic jump is initiated. Inertia of the flow carries it over

the top and it can continue again but at a lower flow velocity until the bed increases in slope again and the flow becomes supercritical again (Figure 8B).

If the flow slows down sufficiently the inertia is no longer enough to carry it over the top and the hydraulic jump gets pushed upstream due to the backwater effect. Here it meets the incoming supercritical flow that does not suffer from this effect and the result is that the hydraulic jump gets pushed onto the supercritical flow and a submerged jump forms. This is a cyclic step (Figure 8C).

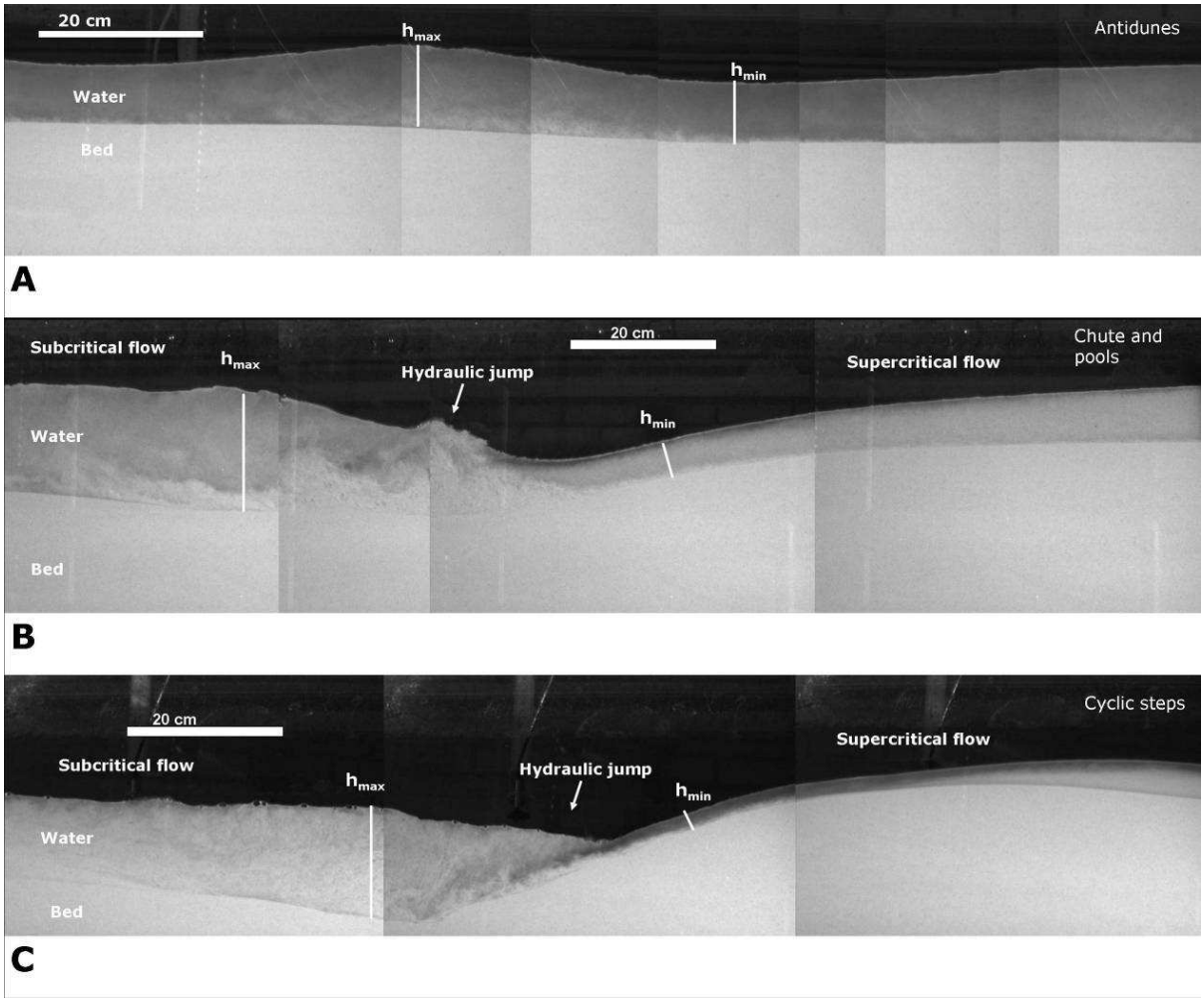

Figure 8 *Results from three different experiments characterising each of the three different types of bedform formed during the experiments. A: Antidunes. B: Chute and Pool. Hydraulic C: Cyclic step.*

Since the criticality of a flow is defined by the Froude number we used it to describe the flow. To determine the Froude number we need to know 3 parameters: *u, g* and *h*
From the images, supplied by the camera, the waterdepth was determined at a fixed location through time. This gives us h by counting pixels. We also continuously measured the discharge. Using the waterdepth at a given location and the constant width of the flume (0.485 m) we can determine the depth-averaged flow velocity at that location (*g* is taken to be constant at 9.81 m/s^2).

The presence of hydraulic jumps forces us to determine waterdepth at more than one location. The choice was made for h_{min} and h_{max} (Figure 8) in order to calculate the Froude numbers before and after the jump. The resulting Froude numbers are plotted in Figure 9. The different runs are grouped by the presence and nature of the hydraulic jump and the corresponding classification.

		Raw data					Calculated			
Run	Result	Duration	D_{50} (μm)	D_{90} (μm)	D_*	Q_{avg} (m^3/hr)	h_{min} (m)	h_{max} (m)	Fr_{min}	Fr_{max}
1	Cyclic steps	123 min	190	270	3.03	64.76	0.020	0.129	0.30	5.32
2	Chute and Pools	120 min	190	270	3.03	80.01	0.032	0.076	0.68	2.54
3	Antidunes	124 min	190	270	3.03	156.51	0.063	0.107	0.87	1.44
4	Upper plane bed	123 min	190	270	3.03	244.6	0.142	0.144	0.68	0.68
5	Cyclic steps	121 min	190	270	3.03	138.12	0.048	0.193	0.34	2.43
6	Chute and pools	120 min	190	270	3.03	132.46	0.048	0.132	0.51	2.21
7	Antidunes	90 min	190	270	3.03	230.1	0.067	0.111	0.88	1.27
8	Cyclic steps	92 min	425	1900	6.77	180.23	0.033	0.165	0.31	3.71
9	Chute and Pools	90 min	425	1900	6.77	162.11	0.057	0.164	0.52	2.59
10	Antidunes	77 min	425	1900	6.77	147.42	0.066	0.075	1.34	1.61
11	Chute and Pools	126 min	425	1900	6.77	165.87	0.044	0.140	0.67	3.71
12	Chute and Pools	129 min	425	1900	6.77	162.96	0.051	0.169	0.47	2.72
13	Cyclic steps	100 min	425	1900	6.77	146.79	0.043	0.170	0.42	3.13
14	Cyclic steps	65 min	425	1900	6.77	174.67	0.047	0.210	0.35	3.40

Table 1 *Summary of the different runs in the experiment*

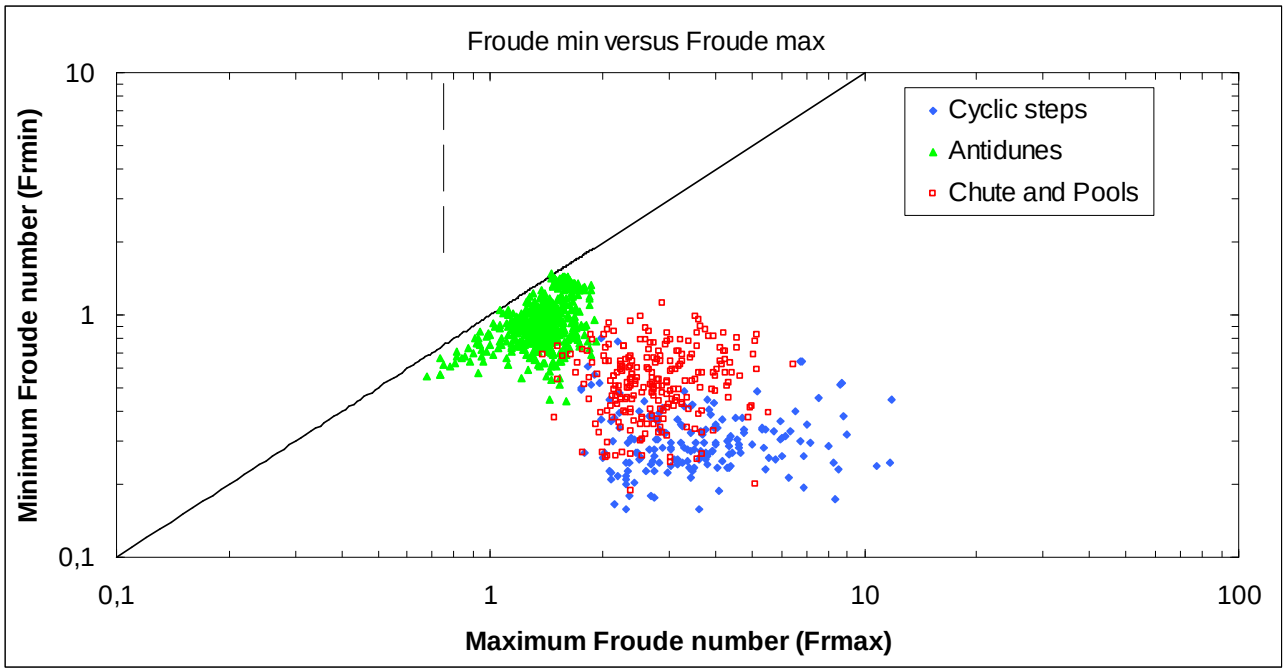

Figure 9 *Plot of Maximum Froude number versus minimum Froude number for each hydraulic jump or the maximum and minimum Froude numbers for a sampling of antidunes. The data points are plotted in the three groups that were determined during the runs themselves as indicated by the presence and nature of hydraulic jumps*

Data Analysis

During the processing of the data from the photographs, it became clear that two distinct morphologies existed in the runs with hydraulic jumps. Cyclic steps have a hydraulic where the incoming flow undercuts the jump itself and a submerged jump is established. The incoming flow comes in at an angle compared to the overall slope of the bed. (Figure 10). Chutes and pools consist of a horizontal jump where the incoming flow is roughly parallel to the overall slope of the bed. (Figure 11).

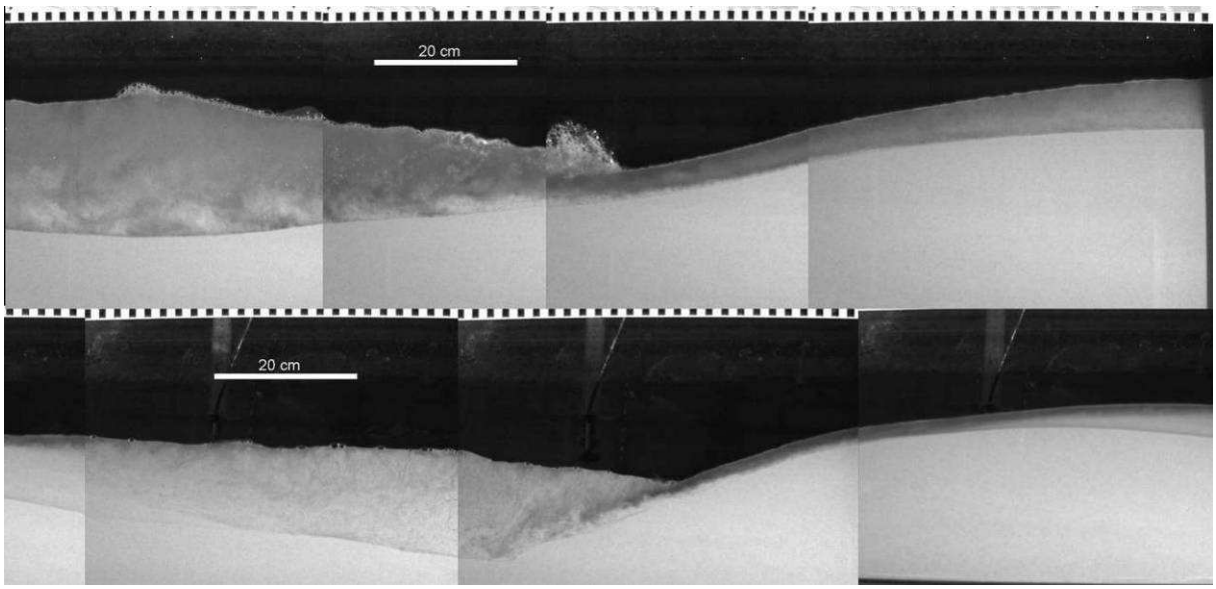

Figure 10 *Composite of cyclic steps occurring during run 6 (Chute and pools, top) and run 1 (Cyclic steps, bottom). Morphologies are the same in that both have a stepped bedform with a submerged hydraulic jump.*

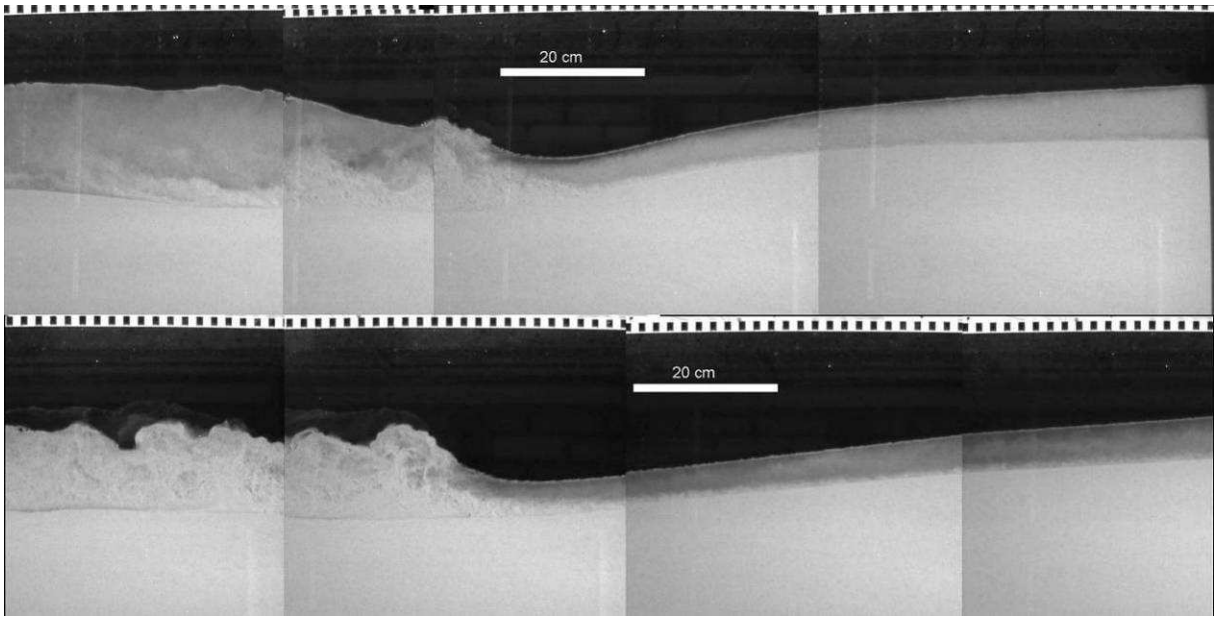

Figure 11 *Composite of Chute and pools occurring during run 5 (cyclic steps, top) and run 6 (Chute and pools, bottom). Both share the same morphology in that there forms a supercritical chute that transitions into a hydraulic jump without undercutting it.*

Data for the different types of bedforms overlap when the Froude number before the jump (Fr_{max}) is plotted against the Froude number after the jump (Fr_{min}) (Figure 9). The hydraulic jumps in the experiments can be divided into two groups: normal jumps and submerged jumps. (Figure 10 and Figure 11) Data from Figure 9 is reclassified using this distinction and is shown in Figure 12. The three different categories are distinct from each other; each plots in its own field.

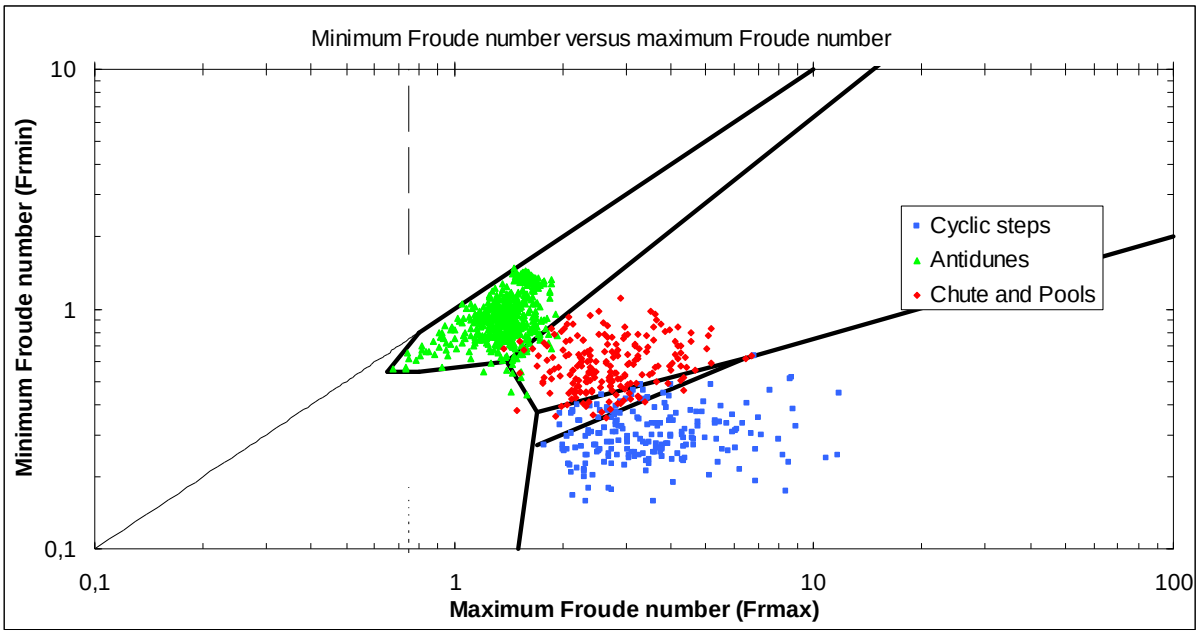

Figure 12 *Plot of Maximum Froude number versus minimum Froude number for each hydraulic jump or the maximum and minimum Froude numbers for a sampling of antidunes In this plot the separate bedforms are subdivided by their morphology, i.e. if there exists a undercutting chute or not.*

Based on these results we make a preliminary upper flow regime stability diagram incorporating the bedforms as determined by their hydraulic jumps and corresponding morphology (Figure 13). The precise relation between Fr_{min} and Fr_{max} is determined by the type of hydraulic jump. By using the ratio between Fr_{max} and Fr_{min} for this diagram we can incorporate the type of hydraulic jump, which heavily influences the type of bedform, into the stability diagram.

This diagram gives good separation for the different bedforms and is a promising start for upper flow regime diagrams. These experiments invite further research in upper flow regime bedforms with emphasis on using sediment with different grain size and distribution. The stability fields provided in Figure 13 should provide a set of boundaries to the paleo-flow conditions. In addition to this it also provides a limit on the Froude numbers represented by the flow and shows that there is a hierarchy in the energy of the bedforms. Cyclic steps have the highest energy, followed by chute and pools and antidunes.

These bedforms can be easily correlated to those found by Alexander et al (2001) and Alexander (2008) in their study on distinctive deposits of upper flow regime bedforms, making it useful to fieldworkers. Antidunes primarily form lenticular laminasets with concave-upward erosional bases (troughs). Sedimentary structures associated with chutes and pools are sets of upstream-dipping laminae and structureless sand. Cyclic steps are related to antidunes as ripples and dunes are related but the resulting sedimentary structures may be distinctly different and considerably variable in character. Further research into the exact sedimentary structures of cyclic steps is necessary.

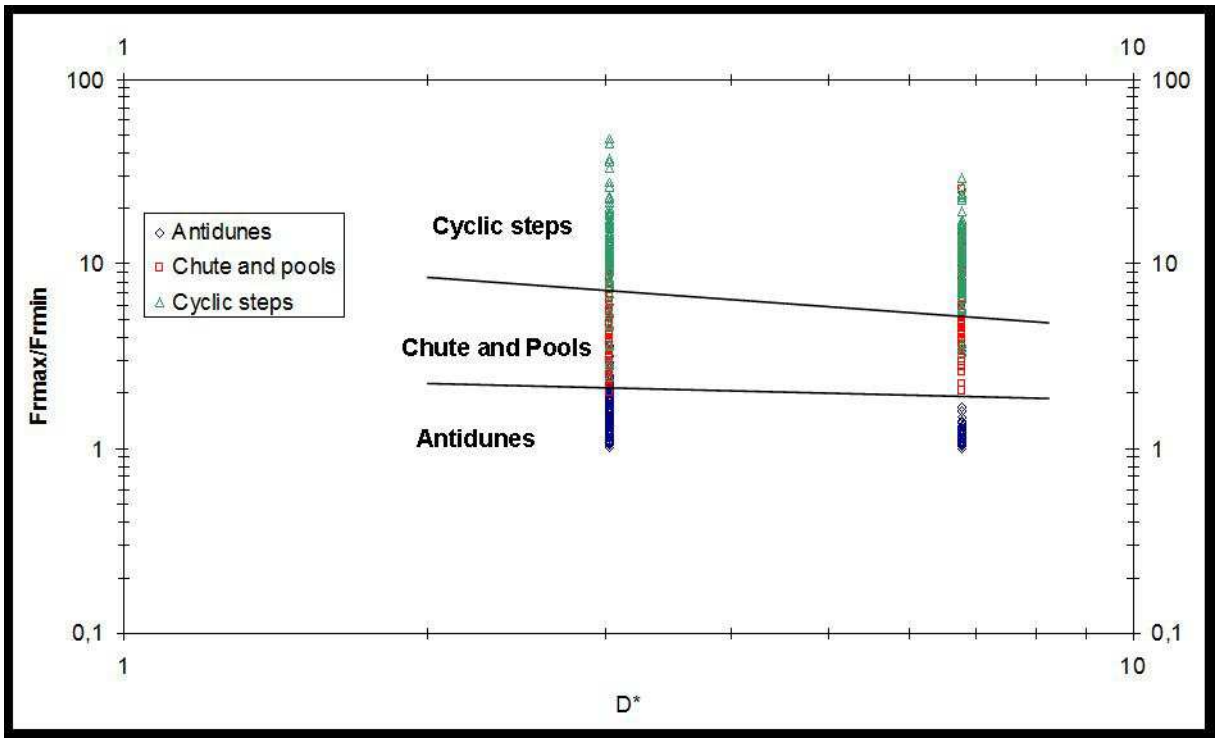

Figure 13 *Ratio of Fr_{max} vs Fr_{min} plotted against the dimensionless grain size. It shows good separation between different bedforms and has potential for stability fields based on this ratio.*

5. Discussion

The stability of upper flow bedforms is determined by the hydraulic jump that shapes them. Supercritical flow over an erodible bed is unstable since the erosive forces are too large to keep a stable bed. Supercritical flow erodes the bed at such a rate that a significant increase in the local slope occurs. This increase in slope causes the flow to accelerate further which in turn increases its erosive power, which is an unstable situation since the local slope can not be increased by sufficient amounts to keep this process going. The resulting slowing of the flow causes a hydraulic jump. After the hydraulic jump the flow starts to accelerate again which will initiate the next jump. This process keeps the whole system of upper flow bedforms stable and makes it possible to create an upper flow stability diagram

Much research has been done on hydraulic jumps (Belanger, 1828, Rajaratnam 1965, Hager 1992) and on lower flow regime bedform stability diagrams (van den Berg and van Gelder 1993, Southard and Boguchwal 1990). These stability diagrams are inherently unsuitable for the upper flow regime, as has been shown in this thesis. Several experiments have been done that studied upper flow regime bedforms (Alexander et al (2001), Taki and Parker (2005), Alexander (2008)) and they established that cyclic steps and antidunes are related to each other in a similar way as dunes and ripples are related – they are bedforms that may occur together or succeed each other and they have some superficial similarity in form. The lack of quantitative data of the flow conditions (such as depth-averaged flow velocity) during these experiments make them unusable for a stability diagram. Their experiments lacked discharge measurements and it was therefore not possible to determine the flow velocity. This is a property that is essential to lower flow stability diagrams. But is it relevant for an upper flow diagram? In order to answer that we need to take a closer look at the determining factor of the upper flow regime: hydraulic jumps.

The morphodynamics of the hydraulic jumps can be described by taking Rajaratnam (1965) into account. He determined a relation between the ratio of the waterdepth before and after the jump

$$\frac{h_2}{h_1} = \frac{1}{2}\left(\sqrt{1+8F_{\max}^2} - 1\right) \qquad \textbf{(6)}$$

where h_1 is waterdepth before the hydraulic jump and h_2 is waterdepth after the jump This works for horizontal (i.e. normal) hydraulic jumps. The supercritical flow is coming down a slope for submerged jumps, so in addition to this relation he proposed an additional one for hydraulic jumps where the incoming flow is angled with respect to the outgoing flow. This was later refined by Hager (1992) to

$$\frac{h_2}{h_1} = \sqrt{2} * 10^{0.027a} * F_{\max} - \frac{1}{2} \qquad \textbf{(7)}$$

where a is the angle of the slope in degrees. Fr_{max} is partly dependent on h_2 while Fr_{min} depends on h_1. As shown by Rajaratnam and Hager, there is a relation between waterdepth and Froude numbers The precise relation over a given jump is dependent on the slope a of the supercritical flow. Since this slope also determines the type of hydraulic jump the relation between Fr_{max} and Fr_{min} is determined by the type of hydraulic jump. The hydraulic jump, in turn, is the factor that separates the different upper flow bedforms from each other. This implies that the formation of upper flow bedforms is determined by the ratio of Fr_{min} and Fr_{max}.

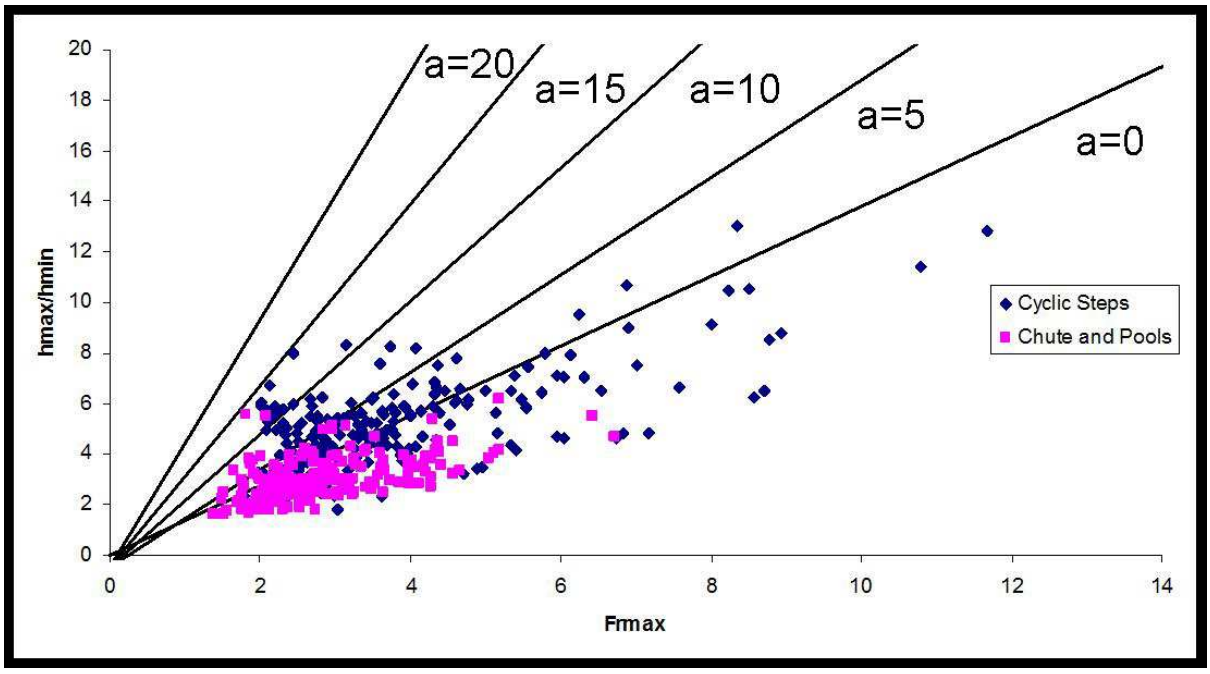

Figure 14. *This graph shows the h2/h1 vs Fr_{max} of cyclic steps (blue) and chutes and pools (pink) as classified by their hydraulic jump and Fr_{max} vs Fr_{min}. The solid lines are the theoretical relation as determined by Rajaratnam 1965 and Hager 1992 with increasing slope (a).*

These two relations are plotted in Figure 14 for several different angles as well as the waterdepth and Froude data for the relevant experiments. This plot shows that the less energetic chute and pool shows a similar relation to the non-sloped variant. The more energetic cyclic steps deviate from the a=0 line indicating that they have a incoming sloped supercritical-flow. This is also taken into account when characterising the different bedforms into the stability diagram.

Hydraulic jumps are the defining factor of upper flow stability diagrams. These jumps are shown here to be dependent on Fr_{min} and Fr_{max}. Therefore the diagram shown in Figure 13 which incorporates both these numbers is a good representation of upper flow bedforms.

Alexander et al (2008), and Taki and Parker (2005) recognized antidunes and cyclic steps as being distinctive in their respective bedforms, with chutes and pools being a subset of cyclic steps. They used the wavelength of the respective bedforms to derive this which is insufficient to describe upper flow regime bedforms. This does not take the intermediate stage of chutes and pools into account they show a varying wavelength over time. Chutes and pools are an important aspect of the upper flow regime since they represent the transitional stage from antidunes to cyclic steps. As Figure 12 shows, chutes and pools are an integral part of the upper flow regime and require different techniques to describe them than solely the wavelength between hydraulic jumps. The ratio between Fr_{min} and Fr_{max} does take the morphodynamics of the hydraulic jump into account and is therefore much more suitable for describing the upper flow regime.

6. Conclusions

From this experimental study several things become clear:

1) Flow parameters differ over the length of the bedform by hydraulic jump.
2) The various bedforms are characterized by various types of hydraulic jump.
3) Each type of hydraulic jump has a characteristic Fr_{max}/Fr_{min} ratio as determined by slope of the supercritical flow.
4) Plots of F_{max}/F_{min} against D^* gives good separation of bedform morphologies. Cyclic steps have the highest energy, followed by chute and pools and antidunes.

These experiments invite further research in upper flow regime bedforms with emphasis on using sediment with different grain size and distribution.

7. Acknowledgements

The experiments done for this thesis were part of an PhD research by Matthieu Cartigny, whose advice greatly helped in establishing a proper set of experiments. I would also like to thank Tony van der Gon Netcher and Henk van der Meer for their help in setting up the experiments and Henk Markies for getting a proper sieve analysis of the sediment. Finally, I'd like to thank George Postma and Peter Morée for helping in finalizing this thesis and making something readable out of it.

8. References

Alexander, J. (2008) Bedforms in Froude-supercritical flow Marine and River Dune Dynamics. *Marine and River Dune Dynamics Proceedings.*

Alexander, J., Bridge, J.S., Cheel, R. & Leclair, S.F. (2001) Bedforms and associated sedimentary structures formed under supercritical water flows over aggrading sand beds. *Sedimentology* **48:** 133-152.

Bélanger, J.B. (1828) "Essai sur la Solution Numérique de quelques Problèmes Relatifs au Mouvement Permanent des Eaux Courantes." ('Essay on the Numerical Solution of Some Problems relative to Steady Flow of Water.') *Carilian-Goeury.*

van den Berg, J.H., & van Gelder, A. (1993) A new bedform stability diagram, with emphasis on the transition of ripples to plane bed in flows over fine sand and silt. *Spec. Publs. Int. Ass. Sediment* **17:** 11-21.

Fagherazzi, S. & Sun, T. (2003) Numerical Simulations of transportational cyclic steps. *Computers and Geoscience.* **29:** 1143-1154.

Gilbert, G.K. (1914) The transportation of debris by running water. *US Geol. Surv. Prof. Pap*. **86:** 263 pp.

Hager, W.H. (1991) Energy Dissipators and Hydraulic Jump. *Kluwer Academic Publishers, Dordrecht.*

Rajaratnam, N. (1967) Hydraulic Jumps. *Advances in Hydroscience,* **4:** 197-280.

Simons, D. B., Richardson, E. V. & Nordin, C. F. (1965) Sedimentary Structures Generated by Flow in Alluvial Channels. *Special Pub. No. 12,* Am. Assoc. Petrol. Geologists.

Simons, D. B. & Richardson, E. V. (1966) Resistance to flow in alluvial channels. *U.S. Geol. Surv. Prof. Paper.* **422-J:** 61 p.

Southard, J.B. & Boguchwal, L.A. (1990) Bed configurations in steady unidirectional water flows. Part 2. synthesis of flume data. *Journal of Sed. Petr.* **60:** 658-679.

Sun, T. & Parker, G. (2005) Transportational cyclic steps created by flow over and erodible bed. Part 2. Theory and numerical simulation *Journal of Hydr. Res.* **43:** 502-514.

Taki, K. & Parker, G. (2005) Transportational cyclic steps created by flow over and erodible bed. Part 1. Experiments. *Journal of Hydr. Res.* **43:** 488-501.

Winterwerp, J.C., Bakker, W.T., Mastbergen, D.R., & van Rossum, H. (1992) Hyperconcentrated sandewater mixture flows over erodible bed. *Journal of Hydraulic Engineering* **119:** 1508-1525.

Yarnell, D.L. (1934b). Bridge piers as channel obstructions. *Tech. Bull. 442, US Department of Agriculture, Washington DC.*

Appendix A

An EMS-probe was used to check the depth-averaged flow velocity measured using the discharge and waterdepth derived from the photos. The values were within the error range of the EMS-probe (Figure 15). The EMS-probe was not used in the other experiments because the height of the bed continuously changes during most runs so it could not be kept at the optimum depth for depth-averaged velocity measurements.

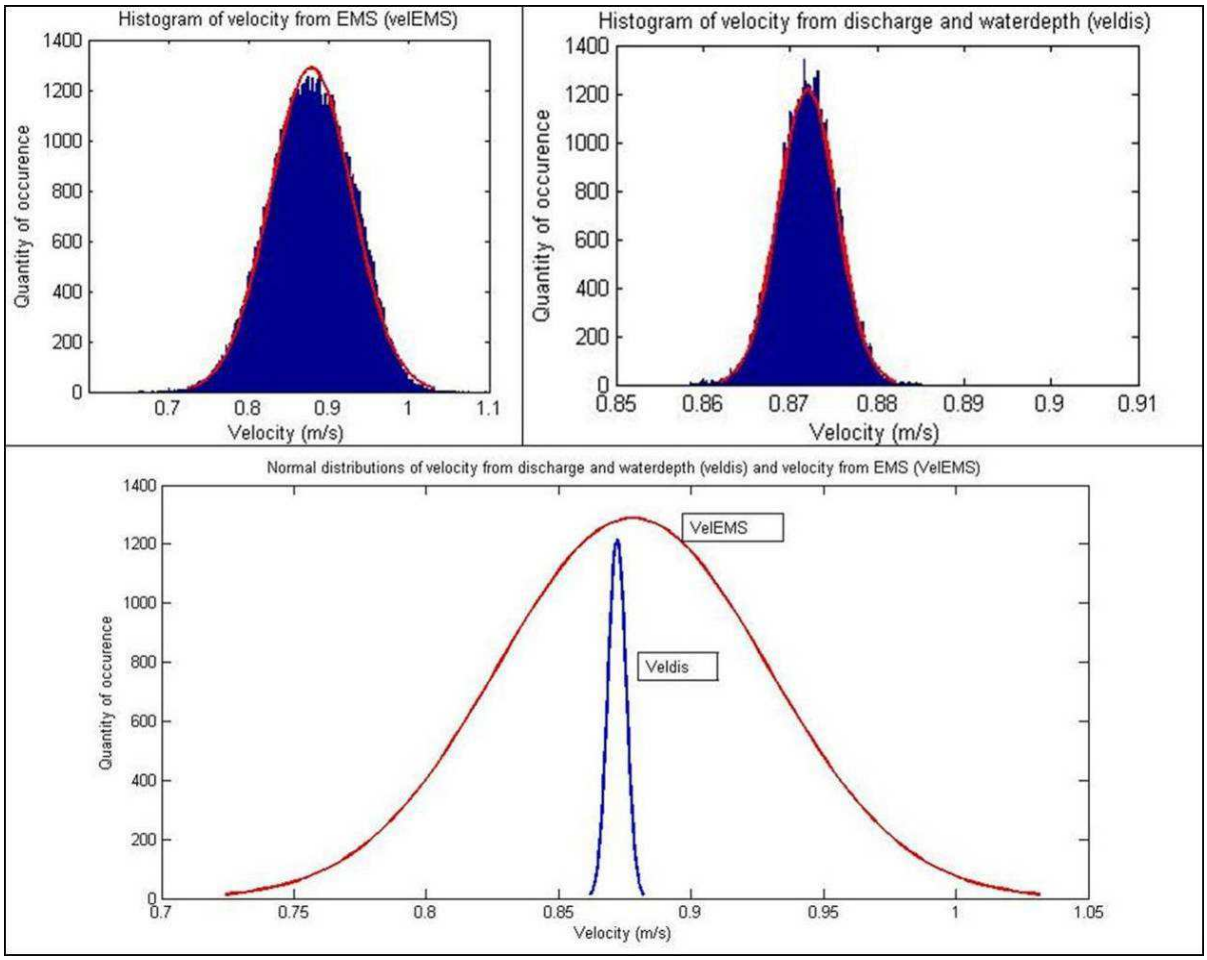

Figure 15 *Top left: histogram of the flow velocity as determined by the EMS-probe, the red line is the corresponding normal distribution. Top right: histogram of flow velocity as determined by the discharge meter and waterdepth: red line is, again, the corresponding normal distribution. Bottom: Both normal distributions in one plot. Velocity determined by discharge is much more accurate.*